ATMOSPHERIC AND OCEANIC SCIENCE LETTERS, 2010, VOL. 3, NO. 5, 1–8

Marine Atmospheric Boundary Layers Associated with Summer Monsoon Onset over the South China Sea in 1998

WANG Dong-Xiao[1], ZHOU Wen[2], YU Xiao-Li[1,3], XIE Qiang[1], and WANG Xin[1,2]

[1] *Key Laboratory of Tropical Marine Environmental Dynamics, South China Sea Institute of Oceanology, Chinese Academy of Sciences, Guangzhou 510301, China*
[2] *Guy Carpenter Asia-Pacific Climate Impact Centre, School of Energy and Environment, City University of Hong Kong, Hong Kong, China*
[3] *Weifang Marine and Environment Monitor Center, Weifang 261401, China*

Received 21 July 2010; revised 8 September 2010; accepted 8 September 2010; published 16 September 2010

Abstract The variations of the marine atmospheric boundary layer (MABL) associated with the South China Sea Summer Monsoon were examined using the Global Positioning System (GPS) sounding datasets obtained four times daily during May-June 1998 on board Research Vessels Kexue 1 and Shiyan 3. The MABL height is defined as the height at the lowest level where virtual potential temperature increases by 1 K from the surface. The results indicate that the MABL height decreased over the northern South China Sea (SCS) and remained the same over the southern SCS, as sea surface temperature (SST) fell for the northern and rose for the southern SCS after the monsoon onset. Over the northern SCS, a decrease in both the SST and the surface latent-heat flux after the onset resulted in a reduction of the MABL height as well as a decoupling of MABL from clouds. It was found that MABL height reduction corresponded to rainfall occurrence. Over the southern SCS, a probable reason for the constant increase of SST and surface heat flux was the rainfall and internal atmospheric dynamics.

Keywords: monsoon onset, marine atmospheric boundary layer height, atmosphere internal dynamics, SST
Citation: Wang, D.-X., W. Zhou, X.-L. Yu, et al., 2010: Marine atmospheric boundary layers associated with summer monsoon onset over the South China Sea in 1998, *Atmos. Oceanic Sci. Lett.*, **3**, ***.

1 Introduction

Significant gradients in the profiles of virtual potential temperature (θ_v) and specific humidity (q) are first detected in the top of the marine atmospheric boundary layer (MABL). Studies on the general characteristics of the MABL are limited due to the lack of ship-time. it was found that weakened (intensified) vertical shear within the MABL is consistent with enhanced (reduced) vertical mixing (Hashizume et al., 2002), which leads to accelerating (decelerating) surface wind over warm (cold) sea surface temperatures (SSTs).

The mixed layer height (MLH), a quantitative measurement of MABL, is defined by a layer with uniform θ_v in the lower part of the MABL (Yin and Albrecht, 2000; Manghnani et al., 2000; Zeng et al., 2004). The MLH in the vicinity of an oceanic front was found to scale with the friction velocity and the Coriolis parameter (Rogers, 1989). Further, it was found that a well-mixed layer capped by a cloud can be maintained if the cloud layer is not eroded by entrainment. Subrahamanyam et al. (2002) studied the variability of the MLH over the western tropical Indian Ocean and central Arabian Sea. During the entire cruise, they observed typical daytime convective MLH at 1400 local time in the range of 200–900 m. Shallow MLHs were also observed over the Intertropical Convergence Zone (Subrahamanyam et al., 2003). Rouault et al. (2000) found that enhanced surface stability and suppressed convection caused a reduction of the MLH. Tokinaga et al. (2006) showed that reduced surface sensible-heat flux suppressed the formation of an atmospheric mixed layer.

The onset of the South China Sea summer monsoon (SCSSM) is regarded as an eastward extension of the Indian summer monsoon and the precursor of the East Asian summer monsoon (e.g., Xie et al., 1998; Ding and Liu, 2001; Wang and Lin, 2002; Zhou and Chan, 2005). It is related to changes in the atmospheric condition over the tropics. Liu and Ding (2000) found that the MLH decreased and even disappeared after the SCSSM onset.

In this study, we investigate the MABL response to SST variations by examining an extremely warm SST event（SST > 30°C）during the SCSSM onset in 1998 over the southern SCS. This has never been studied before. The MABL process plays an important role in the air-sea interaction. Ocean surface fluxes are determined by the SST as well as by air temperature, humidity, and wind speed near the ocean surface; all of which are explicitly linked to the MABL processes. A brief description of the data and methods is provided in Section 2. An overview of the MABL structure and its diurnal variation is provided in Section 3 followed by detailed comparisons of MABL height variation before and after the 1998 SCSSM onset in Section 4, and by investigations on possible factors influencing the MABL height in Section 5. Conclusions and discussions are provided in Section 6.

2 Data and methods

The field observations during the South China Sea Monsoon Experiment (SCSMEX) provide opportunities

Corresponding author: WANG Dong-Xiao, dxwang@scsio.ac.cn

to better understand the activities during the SCSSM. The SCSSM in 1998 started over the northern SCS on 17 May and the rainy season over South China commenced at the same time. During 22 to 26 May, the monsoon over the central and southern SCS commenced. By the end of June, the monsoon prevailed over the entire SCS (Liu and Ding, 2000; Ding et al., 2004). We define the monsoon onset dates in 1998 as 17 May over the northern and 22 May over the southern SCS following the Liu and Ding (2000) study. Surface datasets (wind speed, air temperature, and relative humidity at the air-sea interface) from the Surface System at the National Center for Atmospheric Research, in situ SST, and conductance-temperature-depth measured at R/V (Research Vessel) Kexue 1 (6°15'N, 110°E) and R/V Shiyan 3 (20°29'39"N, 116°57'48"E) were used in this study. The observation periods in the two R/Vs were from 5 to 25 May, and from 5 to 24 June. The surface heat fluxes were calculated using data recorded by the two R/Vs. The precipitation data were from the Tropical Rainfall Measuring Mission (TRMM) GPCP-Huffman 1DD (Global Precipitation Climatology Project-1 Degree Daily Precipitation Estimate). The TRMM Microwave Imager (TMI) measured SST is 3-day mean and has a resolution of 0.25°×0.25°. The reanalysis data in the SCSMEX dataset, with four times daily from May to August, was used to understand the water-vapor divergence.

The Global Positioning System (GPS) sounding data (measured at 0000, 0600, 1200, and 1800 UTC) obtained from the balloon-borne Väisälä Sounding System were used to study the vertical structures of air temperature, relative humidity, wind direction, and wind velocity in the lower troposphere. There are a total of 154 soundings taken by R/V Shiyan 3 and 152 soundings by R/V Kexue 1. In addition, there are 108 soundings in Dongsha Island (20°42′N, 116°43′E). The soundings can reach 20 km above the surface. The data was sampled every second and every 5–25 m in the vertical depending on the balloon's lifting velocity. To preserve the thermodynamic profiles of each individual sounding, this study interpolated the data onto 5-m intervals (Manghnani et al., 2000). After interpolation, q and θ_v were estimated using the following equations:

$$q = 0.622\frac{e}{(p-0.378e)},$$

$$\theta_v = \theta(1+0.61r),$$

$$\theta = T(\frac{p_0}{p})^K,$$

$$Z_c = Z - Z_0 = 123(T_0 - T_{d0}),$$

where e, r, p, θ, C_p, Z, Z_c, T_0, and T_{d0} are the water-vapor pressure (hPa), mixing ration (g kg^{-1}), pressure (hPa), potential temperature (K), specific heat at a constant pressure, the altitude above 1000 Pa, the lifting condensation level (LCL) height, temperature and dew point temperature (K) at the surface, respectively. In addition, K and p_0 are a constant parameter and sea level pressure (also constant).

3 MABL structure and its diurnal variability

Figure 1 depicts the difference of TMI's SST over the SCS before and after the SCSSM onset in 1998. After the onset, the SST over the northern SCS decreased dramatically, whereas the SST over the southern SCS increased steadily. Negative SST anomalies (–2°C to –0.5°C) over the northern SCS and positive SST anomalies (0.5°C to 1°C) over the southern SCS reflected different ocean responses during the SCSSM onset. The SST patterns indicate that the warmer SSTs mainly occurred over the central and southern SCS after the onset. The in situ observations indicated similar results as the TMI dataset.

The MABL height is defined as the height of the lowest level where θ_v increases by 1 K from the surface (Tokinaga et al., 2006). To study the features of the lower troposphere, our analysis is confined to an altitude of 2000 m, and the presence of a mixed layer in the lower atmosphere over the SCS is an important feature. Since there is a friction layer above the surface, the ABL top at this level is defined as the lowest level where q_v increases by 1 K from an altitude of 25 meters. This is slightly different from the Tokinaga et al. (2006) study where the equation is $\theta_v(z)$–$\theta_v(z$=25)=1 K. The profiles of θ_v and q on 7 May and 22 June indicated that both θ_v and q were constant within the mixed layer (Fig. 2). On 7 May, the MABL height reached its maximum at 0600 UTC (1400 LST); and its minimum at 1800 UTC. The MABL height on 22 June also reached its maximum at 0600 UTC; however, it retreated to its minimum six hours earlier than that on 7 May at 1200 UTC (2000 LST). Significant diurnal cycles of the MABL height were often evident over both the northern and southern SCS before the SCSSM onset. However, after the SCSSM onset, the diurnal cycles were inconspicuous, or disappeared over both regions

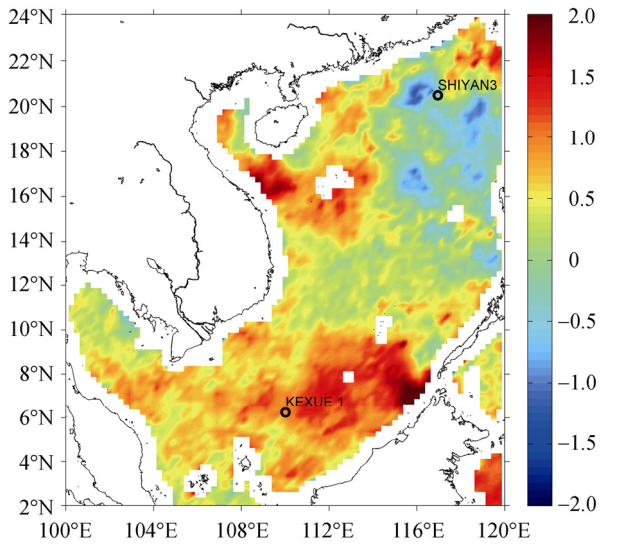

Figure 1 SST difference obtained by using 15-day averages before and after the SCSSM onset. The 1998 SCSSM broke out on 22 May. The locations of R/V Kexue 1 (south) and R/V Shiyan 3 (north) are indicated by circles.

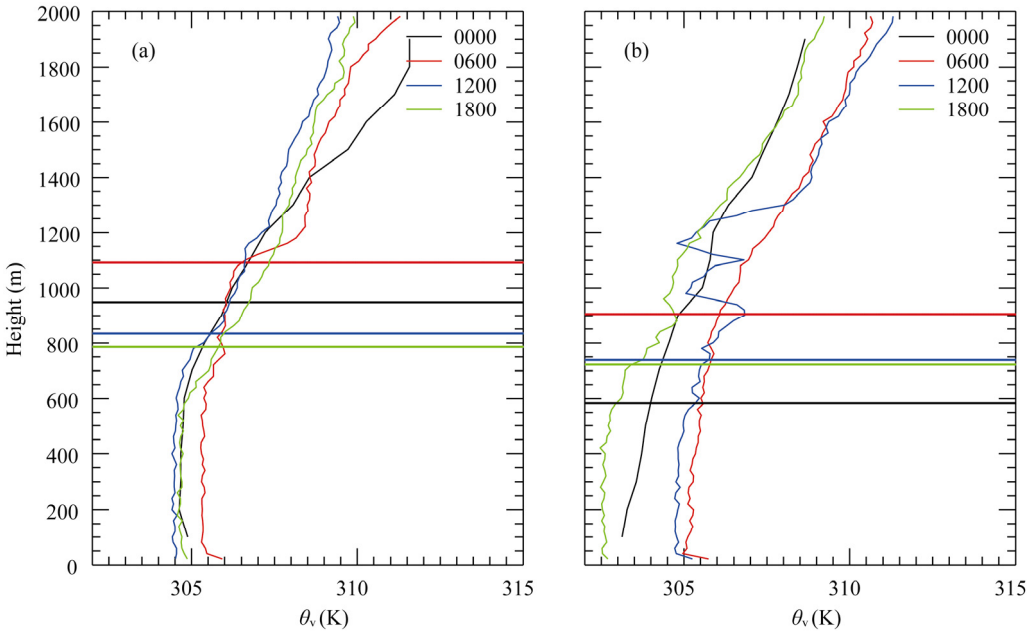

Figure 2 Profiles of the virtual potential temperature at 0600, 1200, 1800, and 2400 UTC on: (a) 7 May 1998 and (b) 22 June 1998. The horizontal lines represent the corresponding MABL heights.

of the SCS. This is consistent with the result obtained in the Webster et al. (1996) study in which the diurnal cycle of the MABL height was attained under calm and clear sky conditions. The strong synoptic activity and increaseing cloudiness after the monsoon onset may be the primary reason for damping the diurnal cycle.

4 MABL height behavior during the SCSSM onset

The sounding profile represents a point measurement deployed from R/V Shiyan 3 and R/V Kexue 1. Significant variability of the MABL height occurred during the observation period. The mean MABL height over the northern SCS before the SCSSM onset (averaged from 5 May to 17 May) was as high as about 760 m; after the onset, it decreased to as low as 540 m, concurring with rapid SST decrease (Fig. 3a). The reduction is about 29%. The mean MABL height over the southern SCS before the monsoon onset (from 5 May to 22 May) was 820 m; after the onset, it decreased slightly to 790 m (Fig. 3b). The reduction over the southern SCS in terms of the mean is only 4%. As compared to the northern SCS, SST over the southern SCS increased after the SCSSM onset. Over the Dongsha Island, a decrease in MABL height by about 90 m, or about 16% after the onset was also found, (Fig. 3c). The MABL height at 0600 UTC is also compared in three places (northern SCS, southern SCS, and Dongsha Island), and results indicate that the MABL over the southern SCS is maintained after the monsoon onset, while it decreased dramatically over the northern SCS and Dongsha Island (Fig. 3d).

Scatter plots of the MABL height and SST are shown in Fig. 4. Over the northern SCS, the MABL height was linearly correlated with local SST with a correlation of 0.43 (pre-monsoon) and 0.44 (post-monsoon) (with a 95% significant confidence level of 0.23; Fig. 4). The linear correlation indicates that a higher (or lower) MABL was associated with warmer (or colder) SST. In contrast, over the southern SCS the correlation coefficient of the MABL height with SST is –0.04. Before the SCSSM onset, the SST varied from 29°C to 30°C and the MABL height changed from 600 m to 1000 m. After the onset, the SST increased to about 31°C, and the mean MABL height decreased to about 30 m. No significant correlation was found over the southern SCS. The correlation between latent-heat flux and MABL height was also studied. The linear correlation between latent-heat flux and MABL height was applicable over the northern SCS (Fig. 4c); however, over the southern SCS, after the SCSSM onset, MABL height variability was not influenced directly by the latent-heat flux (Fig. 4d). The different variability of the MABL height over the northern (and southern) SCS will be discussed below.

5 Factors influencing the MABL development

Previous studies have found that the latent-heat flux and air-sea temperature difference might influence the MABL height. The MABL response to a strong SST gradient across the warm Agulhas current was studied by Rouault et al. (2000). They found that surface heat fluxes increased by over 200 W m^{-2} from the shelf to the current, and a characteristically stable boundary layer over the cool shelf waters was replaced by an unstable convective boundary layer over the current. Using an operational general circulation model, Sam et al. (2007) found that spatial and temporal growth of the coastal atmospheric

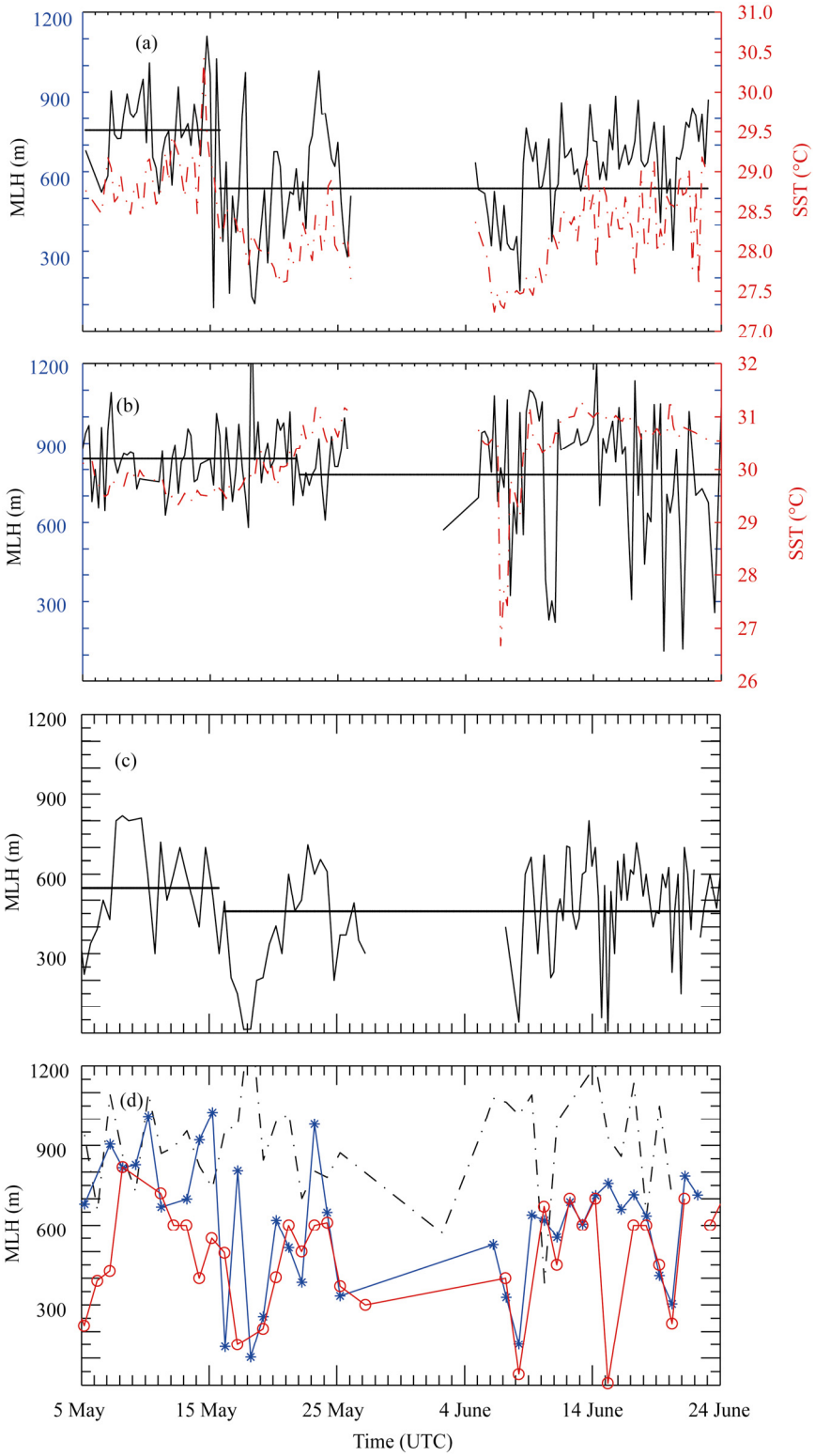

Figure 3 Temporal variation of the MLH and SST at: (a) northern SCS, (b) southern SCS, (c) MLH in Dongsha Island, and (d) MABL height at 0600 UTC. A *t*-test was used to determine the average height during each period. All meet the 95% confidence levels.

boundary layer height was well corroborated with the latent-heat flux during the southwest Indian monsoon period in 2002. Tokinaga et al. (2006) also revealed that MABL height tends to increase as the sea-air temperature difference or the surface turbulent heat flux increases.

The structure and evolution of the MABL are associated with surface sensible-heat and latent-heat fluxes, longwave and shortwave radiations, aerosol concentra-

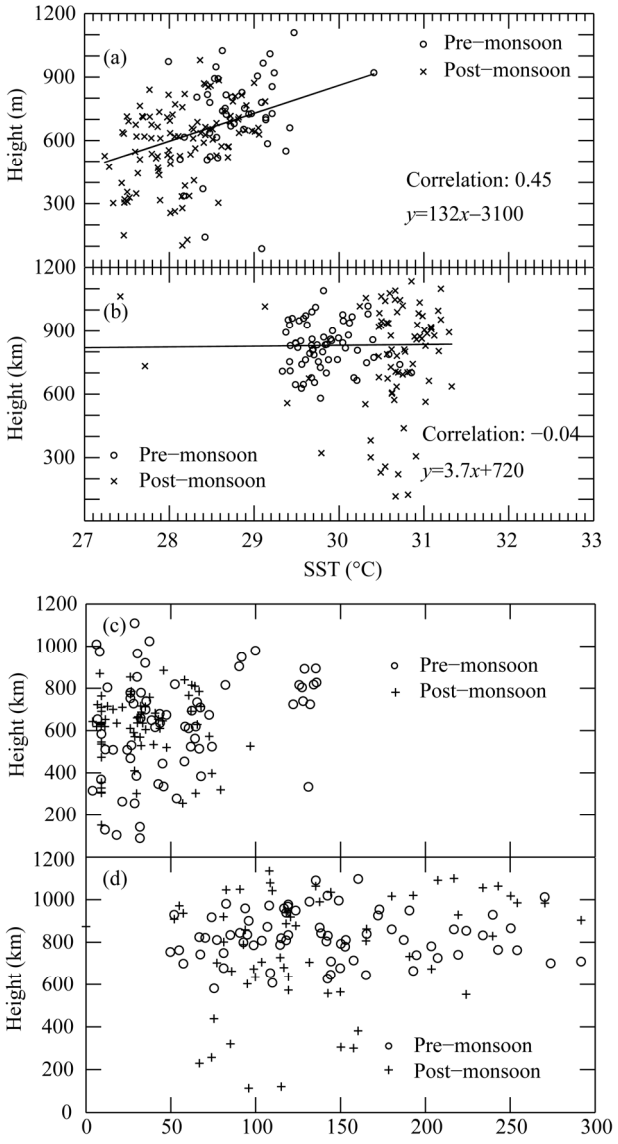

Figure 4 Scatter plots of the MABL height (m) with respect to SST (°C) over: (a) northern SCS, (b) southern SCS, and Scatter plots of the MABL height (m) with respect to latent-heat flux (W m^{-2}) over (c) the northern SCS and (d) the southern SCS.

tions, vertical wind shear, cloud-top entrainment, etc. Limited by observations, we can only discuss the following variables and the possible reasons for their relation to the MABL height. The previous findings are conformed over the northern SCS. The solar radiation over the entire SCS remained uniform except over the northern SCS from 15 to 20 May, and from 2 to 10 June, when it decreased by half (Fig. 5c). The vertically integrated water-vapor contents in the lower atmosphere at the two sites were different (Fig. 5d). Before the SCSSM onset, it was 1–2 g kg^{-1} larger on average over the southern SCS than over the northern SCS; after the onset, it was similar at the two sites despite the fact that the latent-heat flux was larger over the southern SCS. The specific humidity dropped by 2–3 g kg^{-1} over the southern SCS after the onset of monsoon. The vertical wind shear from the surface to the top of the mixed layer had slight changes before and after the SCSSM onset over the whole SCS (Fig. 5e). Both before and after the SCSSM onset, correlation between the MABL height and the variables (relative humidity, surface wind speed, and surface pressure) is not very close. It reveals that the MABL height was not very dependent on the specific humidity.

Over the northern SCS, the sensible heat flux is positive before, and soon after the monsoon onset; there is a small negative sensible heat flux on 20 May to 10 June, and after that, the sensible heat flux is also negative (Fig. 6). The reverse sign of the sensible heat reveals that the atmospheric energy goes through different dynamics: the air begins to transmit energy to the ocean. Without the energy supply, the MABL height decreases. Over the southern SCS, the sensible heat flux is negative before the onset of monsoon, which is contrary from the northern SCS, and after the monsoon onset, the sensible heat flux increases to 80 W m^{-2}, which is twice that of the pre-monsoon. The air above the warm water gains this energy and transfers it upwards maintaining the MABL height.

Internal atmospheric dynamics include the processes of entrainment of temperature inversion and cloud-top capping, among others. The MABL height and the altitude of the LCL are shown in Fig. 7, as the latter is often considered to be the height of the cloud base. Over the northern SCS, from 17 May to 10 June, the difference between the altitude of the LCL and the MLH was small, indicating a possibility of decoupling between the mixed layer and the clouds (Manghnani et al., 2000). However, before the onset of monsoon over the northern SCS, MABL height was greater than the altitude of the LCL, implying saturation in the upper portion of the mixed layer (Manghnani et al., 2000). Over the southern SCS, MABL height was greater than the altitude of the LCL during the entire period.

A pronounced phenomenon is that the MABL height variability is related to rainfall. The precipitation in the vicinity of the R/V locations was calculated (Fig. 8). The decreasing MABL occurred during periods of precipitation. It is found that a change in precipitation has a good relationship with a change in MABL height. Over the northern SCS, the rainfall was mostly during late May and early June (the SCSSM onset), accompanied by a decrease in the MABL height (Fig. 8a). The abrupt changes in the MABL height before SST increases between 5 and 10 May does not seem consistent with SST changes over the northern SCS, probably due to the rainfall blur because the precipitation from 10 to 13 May is 15 mm/day. Over the southern SCS, rainfall occurred mostly in June, concurrent with a slight decrease in MABL height (Fig. 8b).

6 Conclusions and discussions

In this study, we compare the spatial and temporal

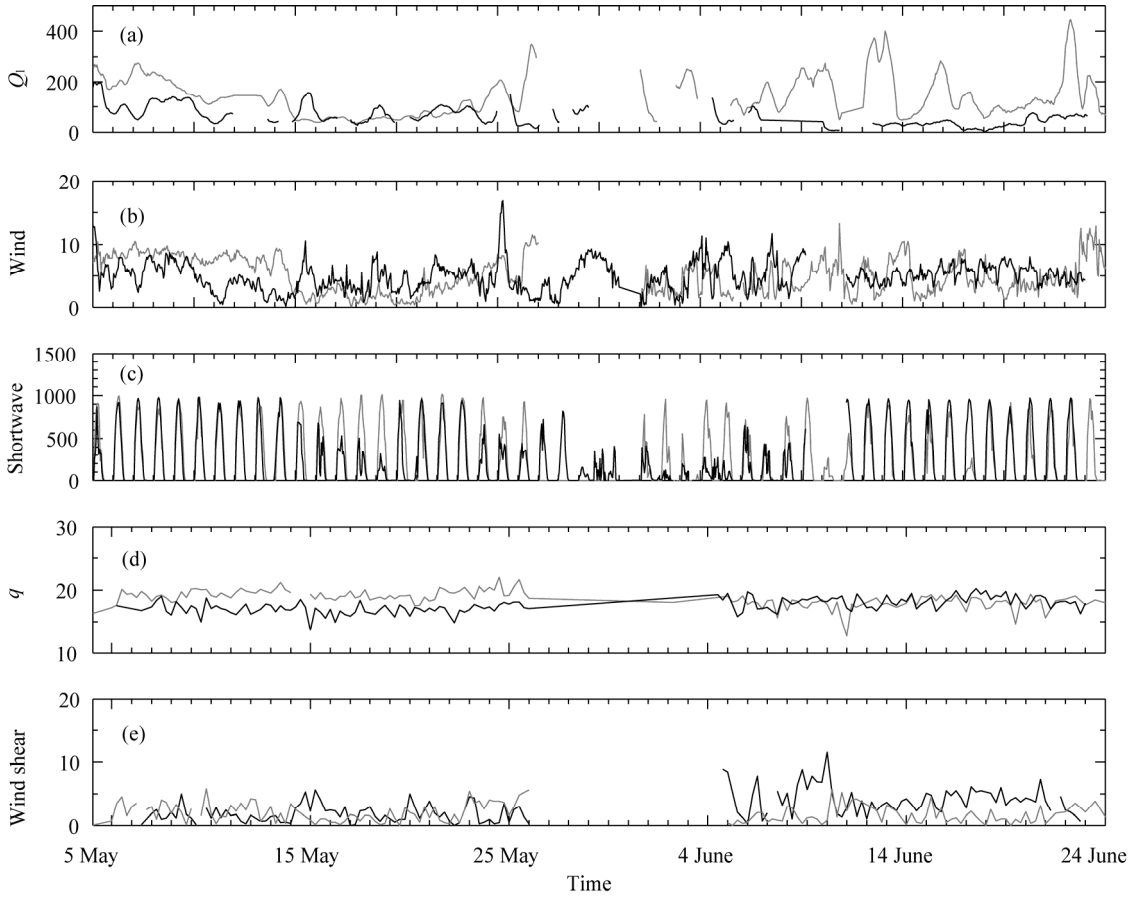

Figure 5 Temporal variation of: (a) latent-heat flux (Q_l; W m^{-2}), (b) surface wind (m s^{-1}), (c) solar radiation (W m^{-2}), (d) average water-vapor content from the surface to 1000 m (g kg^{-1}) over the northern SCS (black line) and the southern SCS (gray line), and (e) vertical wind shear(m s^{-1}) from the surface to the MABL top over the northern SCS (black line) and the southern SCS (gray line).

variability of the MABL height over the northern and southern SCS during the 1998 SCSSM onset. The diurnal cycle of the MABL height over the SCS was evident only before the onset of monsoon. Over the northern SCS, mean MABL height was 760 m before the SCSSM onset, and 540 m after, showing a decrease of 29%. However, over the southern SCS, a decrease in the MABL height after the SCSSM onset was only 4%.

The MABL height reduction over the northern SCS can be attributed to the existence of low-level clouds in the region and the decrease in surface heating. In contrast, the slight change in the MABL height over the southern SCS was due to the fact that the increase in SST and latent-heat flux had counter-balanced the rainfall and internal atmospheric dynamics. The results also indicate that there was more precipitation when the MABL height decreased after the onset, which confirms the inverse relationship between precipitation and MABL height (Johnson et al., 2001; Ciesielski and Johnson, 2009).

The onset of the SCSSM in 1998 was related to the

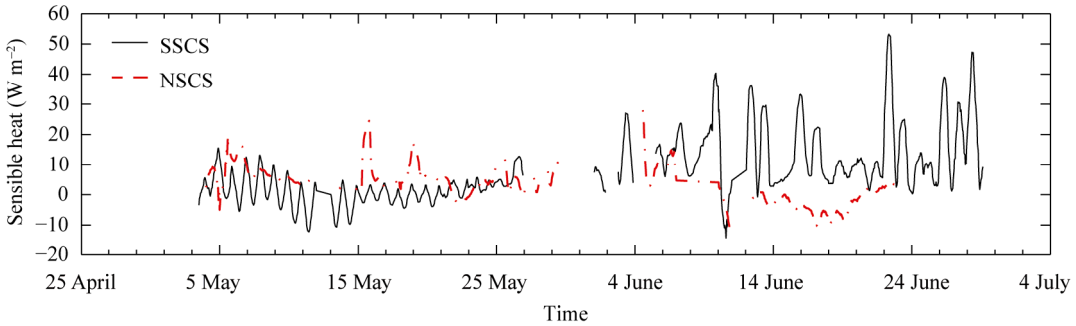

Figure 6 Temporal variation of sensible-heat flux (W m^{-2}) over the northern SCS (red line) and the southern SCS (black line).

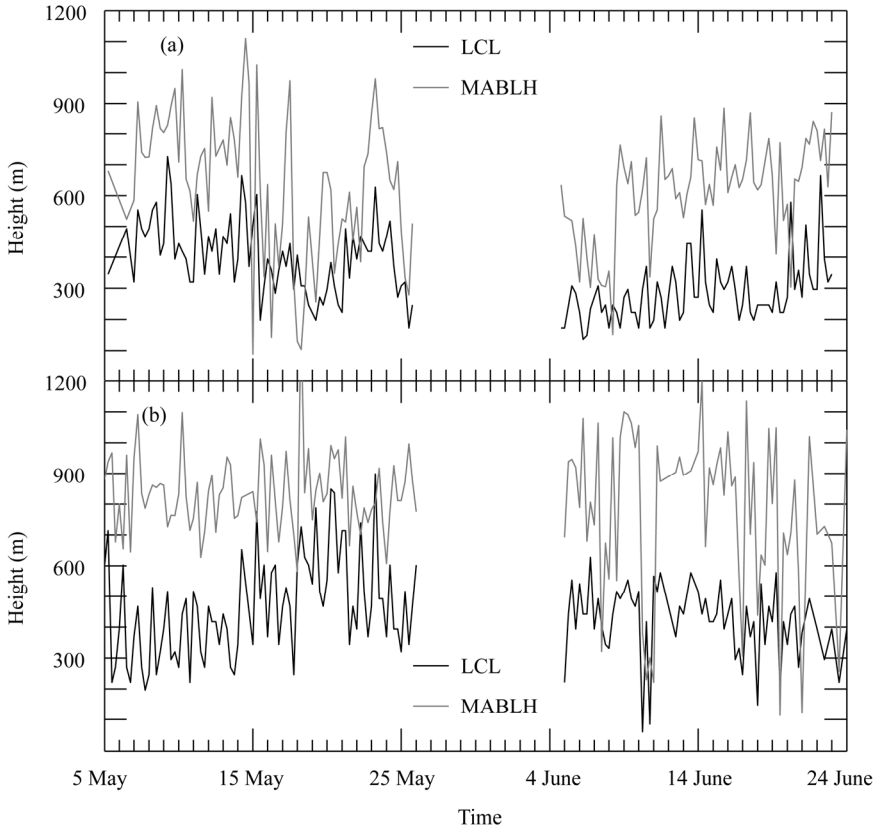

Figure 7 Temporal variations of the MABL height and LCL height over: (a) northern SCS and (b) southern SCS.

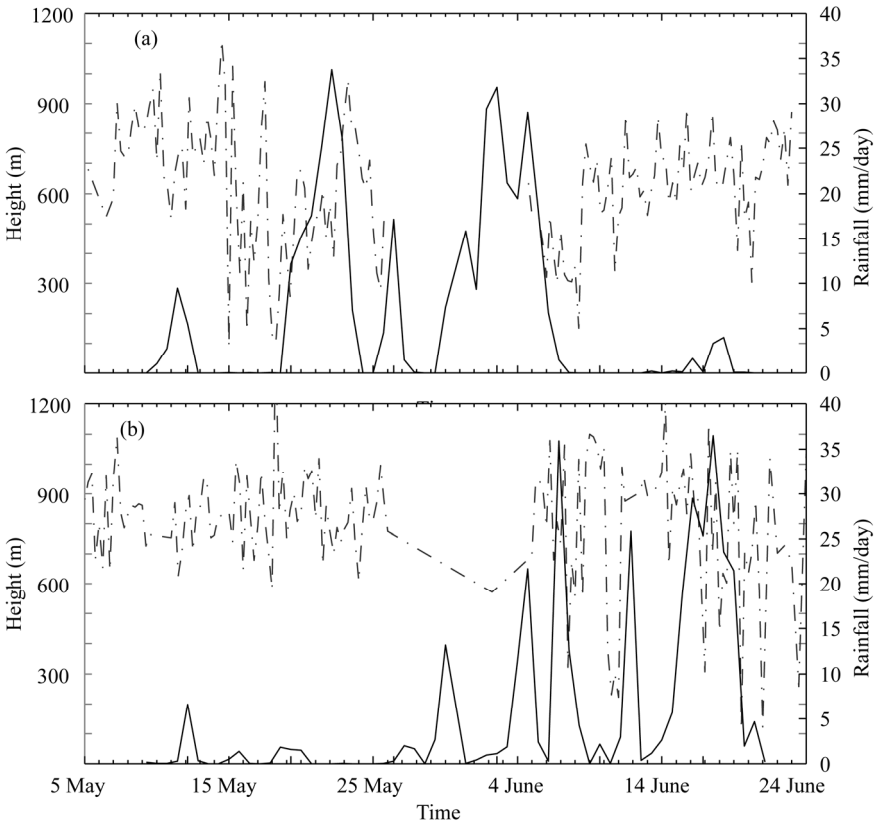

Figure 8 Temporal variation of TRMM precipitation (mm/day) in the vicinity of (a) R/V Shiyan 3 (black solid line) and (b) R/V kexue 1 compared with MABL heights (gray dashed line).

30–60-day oscillation (Madden-Julian Oscillation, MJO) in the SCS. The MJO is known to affect the outbreak of the SCSSM (Mu and Li, 2000). There has been some research on the significant variations of the MABL that are modulated on the intra-seasonal timescale. Due to the limitation of the datasets, we are unable to discuss the influence of the MJO on the MABL. Though the results reported here are from a unique year in terms of the SCS and SST, they are not inconsistent with previous studies. More data are needed to help our understanding of atmospheric stratification in the mixed layer during the onset of monsoon.

Acknowledgements. This work is supported by the Chinese Academy of Sciences (Grant No. KZCX1-YW-12-01), the National Natural Science Foundation of China (Grant Nos. 40733002 and 40876009), and The National Basic Research Program of China (Grant No. 2011CB403504).

References

Ciesielski, P. E., and R. H. Johnson, 2009: Atmospheric mixed layers over the South China Sea during SCSMEX, *SOLA*, **5**, 29–32, doi:10.2151/sola.2009-008.

Ding, Y., C. Li, and Y. Liu, 2004: Overview of the South China Sea monsoon experiment, *Adv. Atmos. Sci.*, **21**, 343–360.

Ding, Y., and Y. Liu, 2001: Onset and the evolution of the summer monsoon over the South China Sea during SCSMEX field experiment in 1998, *J. Meteor. Soc. Japan*, **79**, 255–276.

Hashizume, H., S.-P. Xie, M. Fujiwara, et al., 2002: Direct observations of atmospheric boundary layer response to SST variations associated with tropical instability waves over the eastern equatorial Pacific, *J. Climate*, **15**, 3379–3393.

Johnson, R. H., P. E. Ciesielski, and J. A. Cotturone, 2001: Multiscale variability of the atmospheric mixed layer over the western Pacific warm pool, *J. Atmos. Sci.*, **58**, 2729–2750.

Liu, Y., and Y. Ding, 2000: Evolution of the atmospheric stratification and mixed layer before and after monsoon onset over the South China Sea, *Climatic Environ. Res.* (in Chinese), **5**(4), 459–468.

Manghnani, V., S. Raman, D. S. Niyogi, et al., 2000: Marine boundary-layer variability over the Indian Ocean during INDOEX (1998), *Bound.-Layer Meteor.*, **97**, 411–430.

Mu, M., and C. Li, 2000: On the outbreak of South China Sea summer monsoon in 1998 and activity of atmospheric intraseasonal oscillation, *Climatic Environ. Res.* (in Chinese), **5**(4), 375–387.

Rogers, D. P., 1989: The marine boundary layer in the vicinity of an ocean front, *J. Atmos. Sci.*, **46**, 2044–2062.

Rouault, M., A. M. Lee-Thorp, and J. R. E. Lutjeharms, 2000: The atmospheric boundary layer above the Agulhas Current during alongcurrent winds, *J. Phys. Oceanogr*., **30**, 40–50.

Sam, N. V., U. C. Mohanty, A. Routray, et al., 2007: Variation of coastal atmospheric boundary layer characteristics with convective activity along the west coast of India during the Arabian Sea Monsoon Experiment (ARMEX) 2002, *Nat. Hazards*, **42**(2), 361–378.

Subrahamanyam, D. B., R. Ramachandran, K. S. Gupta, et al., 2003: Variability of mixed-layer heights over the Indian Ocean and central Arabian Sea during INDOEX, IFP-99, *Bound.-Layer Meteor.*, **107**, 683–695.

Tokinaga, H., Y. Tanimoto, M. Nonaka, et al., 2006: Atmospheric sounding over the winter Kuroshio Extension: Effect of surface stability on atmospheric boundary layer structure, *Geophys. Res. Lett.*, **33**, L04703, doi:10.1029/2005GL025102.

Wang, B., and H. Lin, 2002: Rainy season of the Asian-Pacific summer monsoon, *J. Climate*, **15**, 386–398.

Webster, P. J., C. A. Clayson, and J. A. Curry, 1996: Clouds, radiation, and the diurnal cycle of sea surface temperature in the tropical western Pacific, *J. Climate*, **9**, 1712–1730.

Xie, A., Y.-S. Chung, X. Liu, et al., 1998: The interannual variations of the summer monsoon onset over the South China Sea, *Theor. Appl. Climatol*., **59**, 201–213.

Yin, B., and B. A. Albrecht, 2000: Spatial variability of atmospheric boundary layer structure over the eastern equatorial Pacific, *J. Climate*, **13**, 1574–1592.

Zeng, X., M. A. Brunke, M. Zhou, et al., 2004: Marine atmospheric boundary layer height over the eastern Pacific: Data analysis and model evaluation, *J. Climate*, **17**, 4159–4170.

Zhou, W., and J. C. L. Chan, 2005: Intraseasonal oscillations and the South China Sea summer monsoon onset, *Int. J. Climatol.*, **25**, 1585–1609.